Journal of Solid Mechanics Vol. 7, No. 1 (2015) pp. 1-12

# Mixed-Mode Stress Intensity Factors for Surface Cracks in Functionally Graded Materials Using Enriched Finite Elements

J. Sheikhi [1], M. Poorjamshidian [2], S. Peyman [3,*]

[1] *Civil Engineering, Imam Hossein University, Tehran, Iran*
[2] *Department of Mechanical Engineering, Imam Hossein University, Tehran, Iran*
[3] *Instructor, Department of Mechanical Engineering, Imam Hossein University, Tehran, Iran*

Received 15 October 2014; accepted 29 December 2014

**ABSTRACT**

Three-dimensional enriched finite elements are used to compute mixed-mode stress intensity factors (SIFs) for three-dimensional cracks in elastic functionally graded materials (FGMs) that are subject to general mixed-mode loading. The method, which advantageously does not require special mesh configuration/modifications and post-processing of finite element results, is an enhancement of previous developments applied so far on isotropic homogeneous and isotropic interface cracks. The spatial variation of FGM material properties is taken into account at the level of element integration points. To validate the developed method, two- and three-dimensional mixed-mode fracture problems are selected from the literature for comparison. Two-dimensional cases include: inclined central crack in a large FGM medium under uniform tensile strain loading and an edge crack in a finite-size plate under shear traction load. The three-dimensional example models a deflected surface crack in a finite-size FGM plate under uniform tensile stress loading. Comparisons between current results and those from analytical and other numerical methods yield good agreement. Thus, it is concluded that the developed three-dimensional enriched finite elements are capable of accurately computing mixed-mode fracture parameters for cracks in FGMs.



**Keywords:** Mixed-mode; Surface crack; Enriched finite elements

## 1 INTRODUCTION

SINCE the first proposal of Functionally Graded Materials (FGMs) in 1984 by material scientists in Sendai, Japan (Ichikawa, 2000), there have been continuously increasing research and development efforts in the areas of manufacturing, characterization, design, testing, modeling and simulation of FGMs. Although initially the concept was developed as an improved alternative to conventional thermal barrier coatings (TBCs) used in such high temperature applications as those in the areas of aerospace and energy, today FGMs have a broad range of applications including but not limited to biomechanics, automotive, wear resistant equipment and sensors. FGMs are multi-phase materials in which the volume fraction of the constituents in the material varies as a function of position, typically in the thickness direction, to achieve the desired strength and functionalities along the bonding and the free surfaces. For a high temperature application, for example, the material composition may be such that it

* Corresponding author.
*E-mail address:* Jamshidi@ihu.ac.ir (S. Peyman).

contains 100% metal at the bonding interface and 100% ceramic at the coating free surface. Therefore, the mismatch of thermo-mechanical properties near the bond line is minimized, while high temperature, wear and oxidation resistance are still achieved on the exposed surface of the FGM coating. Also, applications of FGMs can be seen where the FGM layer acts as a nonhomogeneous interfacial zone to increase the boding strength and reduce residual stresses [1].

In addition to the material and manufacturing process development efforts for functionally graded materials, significant research has also been taking place in the areas of analytical, numerical and experimental methods to understand the mechanical behavior of FGMs under different geometry and loading conditions. Initial analytical work goes back to Delale and Erdogan, who showed that for a mode-I crack problem in a nonhomogeneous infinite plane the square root stress singularity is conserved and that the effect of the Poisson's ratio on stress intensity factors ($K$) is negligible [2]. Later, Eischen, showed that the nature of stress and strain singularity and the associated first two terms in the asymptotic stress field are the same as those for a crack in isotropic-homogeneous medium [3]. Since then, there have been significant amount of research in the analytical methods area covering also the plane and axisymmetric elasticity problems involving mixed-mode cracks in FGMs and FGM-substrate material systems. See for example [4-6]. These developments laid the foundation for numerical modeling and analysis of cracks in FGMs. Eischen, employed $J_k^*$ integrals using finite elements to evaluate mixed-mode stress intensity factors for cracks in two-dimensional FGM configurations [3]. Gue et al., showed that the standard domain integral is sufficiently accurate when applied to FGM's [7]. Santare and Lambros, Kim and paulino demonstrated the use of graded finite elements for nonhomogeneous materials [8, 9]. Dolbow and Gosz, used interaction energy integral method to compute mixed-mode SIFs for plane problems [10]. Kim and paulino, provide a comparison of different two-dimensional finite element methods to compute the mode-I and mixed-mode SIFs for cracks in FGMs. These included: path-independent $J_k^*$ integrals, modified crack-closure integral method and displacement correlation technique [11]. Anlas et al., and Shim et al., study the $K$-dominance of asymptotic stress fields for different geometry and load configurations by comparing them to the actual stress field obtained from finite element analyses [12, 13].

Although initially most analytical and numerical fracture mechanics studies in FGMs focused on two-dimensional plane problems, more recently solutions for three-dimensional cracks have also been reported in the literature. Walters et al., employed the $J$-integral (Rice, 1968) using a domain integral approach to obtain fracture solutions for semi-elliptical surface cracks contained in FGM structures [14]. Using the displacement correlation technique, Yildirim et al., studied the behavior of a semi-elliptical surface crack in an FGM coating bonded to a homogeneous substrate under mechanical or transient thermal loading conditions [15]. Walters et al., also reported mixed-mode stress intensity factors for three-dimensional cracks in FGMs using a two-state interaction integral method [16].

From above, it is clear that the trend for modeling and simulation of mechanical behavior and cracks in FGMs is going towards general mixed-mode loading conditions in three-dimensions. This, indeed, is a critical need since cracks generally initiate as embedded flaws or surface cracks in a structure and, therefore, mostly require three-dimensional analysis capabilities. Moreover, for cracks in structures such as FGMs that might be exposed to severe thermal gradients and other complex boundary conditions depending on the application, a general three-dimensional analysis capability is unavoidable. Therefore, in this paper, functionally graded enriched finite elements are employed to compute mixed-mode stress intensity factors for three-dimensional cracks contained in FGMs. A general-purpose finite element program, ABAQUS is enhanced to be able to analyze mixed-mode three-dimensional cracks in FGMs. Using enriched finite elements, stress intensity factors for three-dimensional surface and corner cracks (homogeneous-isotropic medium) under mixed-mode loading conditions are also available [17].

The article is organized as follows: First, finite element formulation of the functionally graded enriched finite elements are presented. In the numerical examples section, the problem of a mode-I surface crack in an FGM plate under tensile loading is followed by different cases involving two-dimensional mixed-mode loading conditions. These include: inclined central crack in a large FGM medium under uniform tensile strain loading and an edge crack in a finite-size plate under shear traction load. These cases allow comparisons of mode-I and mode-II stress intensity factors with analytical and numerical solutions available in the literature. To demonstrate the general capability of analyzing three-dimensional mixed-mode loading conditions involving all modes of fracture, a deflected surface crack in a finite-size FGM plate under uniform tensile loading is considered. Through above applications, it is demonstrated that enriched elements are suitable to accurately compute fracture parameters for three-dimensional cracks in FGMs in a straightforward and efficient manner without the need for special finite element meshes and post-processing of the results.

## 2 FINITE ELEMENT FORMULATION

This section details the finite-element formulation of enriched crack tip elements for mixed-mode fracture analyses of three-dimensional cracks in FGMs. Similar to many other studies in the literature, the form of material property gradient functions is selected to be exponential. For the FGM domain shown in Fig. 1 containing an inclined embedded crack, for example, the elastic and shear moduli vary according to:

$$E(x_1) = E_0 e^{\beta x_1} \quad \text{and} \quad \mu(x_1) = \mu_0 e^{\beta x_1} \tag{1}$$

where $\beta$ is a material constant and $x_1$ is the coordinate by which the material property changes according to Eq.(1). $E_0$ and $\mu_0$ are the values of the moduli at $x_1 = 0$. It is noted that the procedure developed takes into account material property variations at individual integration points within an element. In the literature, other methods also exist. Some examples are assigning a constant material property value for a given element based on the coordinate of the element centroid and defining temperature dependent properties such that, when accounted for, it results in the desired material property variation.

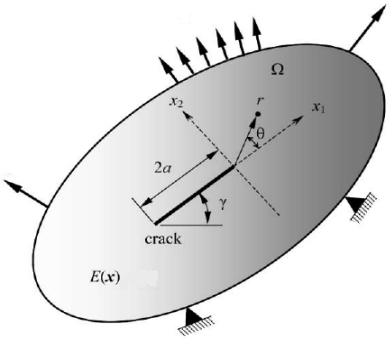


**Fig. 1**
Two-dimensional functionally graded medium containing an inclined crack.

### *2.1 Three-dimensional enriched finite elements for cracks in FGM's*

In this section, the formulation of enriched crack tip elements for three-dimensional mixed-mode crack problems in FGMs is presented. Consider the enriched finite element located along a portion of a crack in an FGM as shown in Fig. 2. The displacements for this element are given by:

$$u(\xi,\eta,\rho) = \sum_{j=1}^{r} N_j(\xi,\eta,\rho)u_j + Z_0(\xi,\eta,\rho)\left\{K_I(\Gamma)F_1(\xi,\eta,\rho) + K_{II}(\Gamma)G_1(\xi,\eta,\rho) + K_{III}(\Gamma)H_1(\xi,\eta,\rho)\right\} \tag{2}$$

$$\vartheta(\xi,\eta,\rho) = \sum_{j=1}^{r} N_j(\xi,\eta,\rho)\vartheta_j + Z_0(\xi,\eta,\rho)\left\{K_I(\Gamma)F_2(\xi,\eta,\rho) + K_{II}(\Gamma)G_2(\xi,\eta,\rho) + K_{III}(\Gamma)H_2(\xi,\eta,\rho)\right\} \tag{3}$$

$$w(\xi,\eta,\rho) = \sum_{j=1}^{r} N_j(\xi,\eta,\rho)w_j + Z_0(\xi,\eta,\rho)\left\{K_I(\Gamma)F_3(\xi,\eta,\rho) + K_{II}(\Gamma)G_3(\xi,\eta,\rho) + K_{III}(\Gamma)H_3(\xi,\eta,\rho)\right\} \tag{4}$$

In Eqs. (2), (3) and (4) $u_j$, $v_j$ and $w_j$ represent the $r$ unknown nodal displacements and $N_j$ ($\xi$, $\eta$, $\rho$) are the conventional element shape functions in terms of the element's local coordinates. $K_I(\Gamma)$, $K_{II}(\Gamma)$, $K_{III}(\Gamma)$ represent the mode-I, -II and -III stress intensity factors varying along the crack front and are defined by the unknown nodal stress intensity factors, $K_I^i, K_{II}^i, K_{III}^i$, and element shape functions $N_i(\Gamma)$ evaluated along the element edge located on the crack front. $Z_0$ is a linear transition function for the elements that surround the crack tip elements and take a value of "1" at surfaces shared with crack tip elements including everywhere in the enriched element, and "0" on faces that are shared with the regular finite elements [18]. For a quadratic hexahedral enriched element, in addition to the 60 unknown nodal displacements, a total of nine (three for each mode) unknown stress intensity factors are also

included in the element formulation. As a result, the unknown nodal displacements and stress intensity factors are solved simultaneously during solution of the system of finite element equations. Therefore, unlike some other methods such as displacement correlation and *J*-integral, enriched finite element method eliminates the need for post-processing the finite element solution to obtain the fracture parameters, which can be quite laborious for a three-dimensional crack problem with arbitrary crack shape contained in a three-dimensional body.

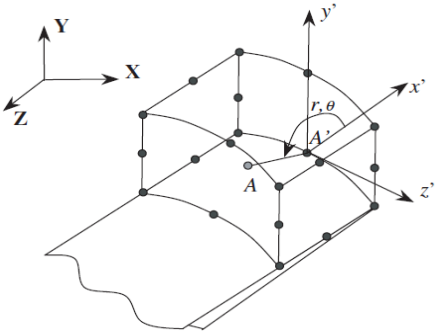


**Fig. 2**
Schematic of a 20-noded enriched finite element located at a portion of an arbitrarily -oriented crack in a functionally graded material.

The functions $F_i$, $G_i$, $H_i$ in Eqs. (2), (3) and (4) are given by:

$$F_i(\xi,\eta,\rho) = f_i(\xi,\eta,\rho) - \sum_{j=1}^{r} N_j(\xi,\eta,\rho) f_{ij} \tag{5}$$

$$G_i(\xi,\eta,\rho) = g_i(\xi,\eta,\rho) - \sum_{j=1}^{r} N_j(\xi,\eta,\rho) g_{ij} \tag{6}$$

$$H_i(\xi,\eta,\rho) = h_i(\xi,\eta,\rho) - \sum_{j=1}^{r} N_j(\xi,\eta,\rho) h_{ij} \tag{7}$$

In Eqs. (5), (6) and (7) $f_i$, $g_i$, $h_i$ ($i$ = 1,2,3) contain the asymptotic displacement functions that are coefficients of the mode-I, -II and -III stress intensity factors with respect to the global coordinate system. The terms $f_{1j}$, $g_{1j}$, $h_{1j}$, $f_{2j}$, $g_{2j}$, $h_{2j}$, $f_{3j}$, $g_{3j}$, $h_{3j}$ are simply constants computed from the $f_i$, $g_i$, $h_i$ functions evaluated at the $j$th node in the element. Hartranft and Sih showed that the crack tip fields along a three-dimensional crack-front in homogeneous materials are the same as those for a two-dimensional crack under plane strain conditions [19]. Also, for two-dimensional cracks in FGMs, Delale and Erdogan, and Eischen, showed that the leading terms in the asymptotic local crack tip fields are the same as those for a corresponding homogeneous-isotropic material [2, 3]. Therefore, the local crack tip displacements for a three-dimensional crack in an isotropic-homogeneous material can be used for cracks in FGMs by taking into account the spatial material property variation. These displacements are given by,

$$\bar{u} = K_I \bar{f}_1 + K_{II} \bar{g}_1, \quad \bar{\upsilon} = K_I \bar{f}_2 + K_{II} \bar{g}_2, \quad \bar{w} = K_{III} \bar{h} \tag{8}$$

where

$$\bar{f}_1 = \frac{1}{2E}\sqrt{\frac{r}{2\pi}}\left(\left(5-3\nu-8\nu^2\right)\cos\left(\frac{\theta}{2}\right)-\left(1+\nu\right)\cos\left(\frac{3\theta}{2}\right)\right) \tag{9}$$

$$\bar{g}_1 = \frac{1}{2E}\sqrt{\frac{r}{2\pi}}\left(\left(9+\nu-8\nu^2\right)\sin\left(\frac{\theta}{2}\right)+\left(1+\nu\right)\sin\left(\frac{3\theta}{2}\right)\right) \tag{10}$$

$$\bar{f}_2 = \frac{1}{2E}\sqrt{\frac{r}{2\pi}}\left(\left(7-\nu-8\nu^2\right)\sin\left(\frac{\theta}{2}\right)-\left(1+\nu\right)\sin\left(\frac{3\theta}{2}\right)\right) \tag{11}$$

$$\overline{g}_2 = -\frac{1}{2E}\sqrt{\frac{r}{2\pi}}\left(\left(3-5\nu-8\nu^2\right)\cos\left(\frac{\theta}{2}\right)+\left(1+\nu\right)\cos\left(\frac{3\theta}{2}\right)\right) \tag{12}$$

$$\overline{h} = \frac{2}{E}\sqrt{\frac{2r}{\pi}}\left(1+\nu\right)\sin\left(\frac{\theta}{2}\right) \tag{13}$$

In Eqs. (8), (9), (10), (11), (12) and (13), $E$ and $\nu$ are the elastic constants evaluated at an arbitrary location in the vicinity of the crack tip based on FGM material gradation and $r$, $\theta$ are measured locally from the crack front as shown in Fig. 2. The relationship between the local crack tip displacement components $\overline{u}_i$, Eqs. (8), (9), (10), (11), (12) and (13), and the global displacements $u_i$ are found through the usual vector transformations. Using index notation

$$u_i = a_{ji}\overline{u}_j \tag{14}$$

where $a_{ji}$ represents the direction cosines between the primed axes and the global axes in Fig. 2, i.e., $a11 = \cos(x', x)$, $a12 = \cos(x', y)$, $a13 = \cos(x', z)$, etc. It should be noted that, for a general three-dimensional problem, the direction cosines used to perform the local-to-global transformations are, in general, different at every point in the enriched element. In addition, for element coordinate values of $\xi$, $\eta$, $\rho$ located at the element nodes, the displacements are simply given by the leading terms in Eqs. (2), (3) and (4), since $F_i$, $G_i$, and $H_i$, Eqs. (5), (6) and (7), are identically zero at these points.

For the cases studied in this paper, the cracks are contained in a graded material. Therefore, elastic modulus and Poisson's ratio in Eqs. (8), (9), (10), (11), (12) and (13) are functions of position and evaluated accordingly for all integration and nodal points during the formation of element stiffness matrices and force vectors of enriched elements.

## 3 NUMERICAL EXAMPLES

In a study (Ayhan), systematic investigations have been made to assess the accuracy of enriched elements when compared to analytical results by changing the mesh refinement near the crack front (*a/S_tip*, where *a* is the crack length and *S_tip* is the crack tip element edge length in planes perpendicular to the crack front) and by turning the transitional enriched elements on and off [17]. This led to the conclusion that transition elements need to be used along with a certain level of mesh refinement near the crack front to compute accurate stress intensity factors. In the same study, using comparable finite element models for surface crack problems in FGMs, very close stress intensity factors have also been computed to those from conventional finite element analyses Yildirim et al., that employed the displacement correlation technique (DCT) [15]. Thus, it is noted that although results from enriched element method and conventional finite element analyses can be close to each other, enriched elements advantageously do not require special meshes, i.e., quarter-point elements, near the crack front and no-post processing of the finite element solution is needed, both of which can be quite laborious for an arbitrarily general three-dimensional fracture problem.

In this section, numerical examples are presented to demonstrate the application of three-dimensional enriched finite elements to mixed-mode cracks in FGMs. First, a mode-I surface crack problem is presented. An inclined central crack in a two-dimensional FGM plate under uniform tension and an edge crack in an FGM plate under shear loading demonstrate accurate computation of mode-I and mode-II stress intensity factors for two-dimensional cracks in FGMs. To show the application of enriched elements on problems in which all three modes of fracture exist, the case of a deflected surface crack in a finite-size FGM plate is presented. All of the results obtained for the above problems are compared with the available solutions in the literature. In a study (Ayhan), other capabilities of enriched finite elements, such as free-surface mesh refinement and being able to prescribe stress intensity factor constrains, were demonstrated on a mode-I surface crack in an FGM plate [17]. It is noted that the finite element models presented in this paper are generated by using ABAQUS and converted into MATLAB for analysis.

*3.1 Fracture analysis of a mode-I surface crack in a finite-thickness FGM plate*

Before the mixed-mode fracture problems, the application of three-dimensional enriched finite elements for a mode-I surface crack (Fig. 3) in an FGM plate is calculated. As can be seen in Fig. 3, the material gradient is in "*x*" direction and the plate is under uniform far-field tensile load. For the problem considered, $a/t = 0.2,\ 0.5,\ 0.8$, $a/c = 1.0,\ 2.0$, $E(t)/E(0) = 5.0$, $\nu = 0.25$.

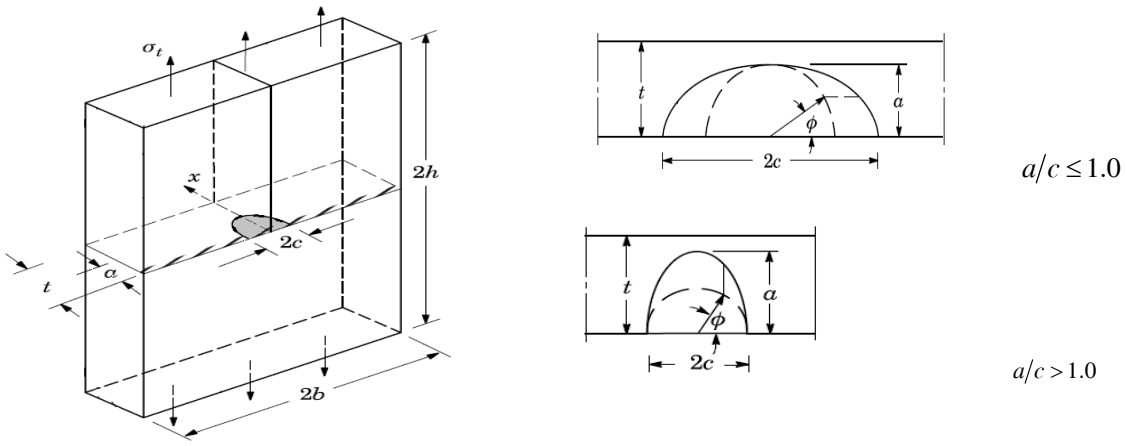


**Fig. 3**
Finite-thickness FGM plate containing a mode-I semi-elliptical surface crack under uniform tension loading.

Fig. 4 shows the mesh details of the finite element model. As can be seen from the figure, only 1/4th of the plate is modeled to take advantage of symmetry in *y* and *z* directions. Along the crack front, 181 nodes and 90 quadratic elements are used. The model has 69257 quadratic elements and 99038 nodes.

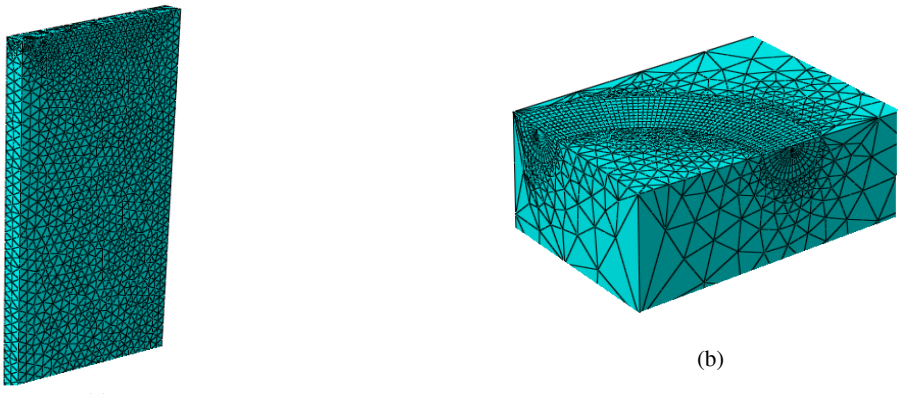

(a) (b)

**Fig. 4**
Finite-element model of FGM plate containing semi-elliptical surface crack, a/t = 0.8, a/c = 1.0 (a) Overall view, (b) Close-up view of the crack region.

Fig. 5 shows comparison of the enriched element solution to the results of Walters et al., (2004) for the same problem [15]. As can be seen from the figure, good agreement is obtained between the enriched element solution and J-integrals for FGM cases. The stress intensity factors are normalized by,

$$K_R = \sigma_0 \sqrt{\frac{\pi a}{Q}} \tag{15}$$

$Q$ is defined by,

$$Q = \begin{cases} 1 + 1.464\left(\dfrac{a}{c}\right)^{1.65} & \dfrac{a}{c} \le 1 \\ 1 + 1.464\left(\dfrac{c}{a}\right)^{1.65} & \dfrac{a}{c} > 1 \end{cases} \tag{16}$$

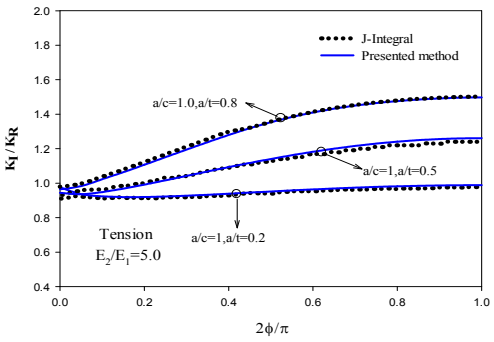


**Fig. 5**
Normalized mode-I stress intensity factors and comparison with *J*-integral.

### *3.2 Inclined central crack in an FGM medium under uniform strain loading*

Fig. 6(a) shows an interior inclined crack of length 2a located with angle $\theta$ in a finite two-dimensional plate, and Fig. 6(b) shows mesh configurations with various crack slopes measured clockwise. Konda and Erdogan [4] have investigated an infinite plate with such a configuration. The applied load corresponds to $\sigma_{22}\left(x_1, 10\right) = \bar{\varepsilon}\bar{E}e^{\beta x_1}$, and such stress distribution was obtained by applying nodal forces along the top edge of the mesh. The displacement boundary condition is prescribed such that $u_2 = 0$ along the lower edge and, in addition, $u_1 = 0$ for the node at the left-hand side. This loading results in a uniform strain $\varepsilon_{11}\left(x_1, x_2\right) = \bar{\varepsilon}$ in a corresponding uncracked structure. Young's modulus is an exponential function of $x_1$, while Poisson's ratio is constant.

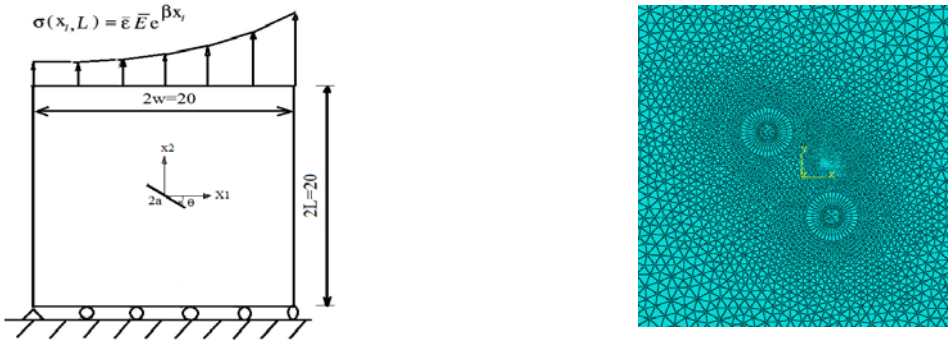


(a) (b)

**Fig. 6**
Finite element model of an inclined crack in an FGM medium, $\theta = 54°$. (a) Overall mesh, (b) Close-up view of crack region.

Table 1. shows the normalized mode-I and mode-II stress intensity factors for $\beta = 0.25$ and different crack orientation angles with respect to the material gradation axis. The normalizing stress intensity factor is defined as $K_0 = \bar{\varepsilon}\bar{E}\sqrt{\pi a}$ . Results of Konda and Erdogan [4] are also included in the table. It is seen that excellent agreement is obtained between the two solutions. Table 2. lists the results for the case of $\beta = 0.50$. Again, good agreement exists between presented methods results and those of Konda and Erdogan [4].

**Table 1**
Normalized mode-I and mode-II stress intensity factors ( $\beta = 0.25$)

| Method | | | $\beta = 0.25$ $K_0 = \bar{\varepsilon}\bar{E}\sqrt{\pi a}$ | | |
|---|---|---|---|---|---|
| | $\theta/\pi$ | $K_I(a)/K_0$ | $K_{II}(a)/K_0$ | $K_I(-a)/K_0$ | $K_{II}(-a)/K_0$ |
| Presented method | 0.0 | 1.221 | 0.0000 | 0.8320 | 0.0000 |
| | 0.1 | 1.119 | -0.3180 | 0.7863 | -0.2252 |
| | 0.2 | 0.809 | -0.5131 | 0.5891 | -0.3972 |
| | 0.3 | 0.430 | -0.5193 | 0.3104 | -0.4213 |
| | 0.4 | 0.140 | -0.3151 | 0.0900 | -0.2811 |
| | 0.5 | 0.000 | 0.0000 | 0.0000 | 0.0000 |
| Konda and ardogan | 0.0 | 1.220 | 0.0000 | 0.8401 | 0.0000 |
| | 0.1 | 1.106 | -0.3150 | 0.7663 | -0.2309 |
| | 0.2 | 0.810 | -0.4942 | 0.5819 | -0.3905 |
| | 0.3 | 0.404 | -0.5231 | 0.2972 | -0.4392 |
| | 0.4 | 0.135 | -0.3045 | 0.0945 | -0.2800 |
| | 0.5 | 0.000 | 0.0000 | 0.0000 | 0.0000 |

**Table 2**
Normalized mode-I and mode-II stress intensity factors ( $\beta = 0.5$)

| Methods | | | $\beta = 0.5$ $K_0 = \bar{\varepsilon}\bar{E}\sqrt{\pi a}$ | | |
|---|---|---|---|---|---|
| | $\theta/\pi$ | $K_I(a)/K_0$ | $K_{II}(a)/K_0$ | $K_I(-a)/K_0$ | $K_{II}(-a)/K_0$ |
| Presented method | 0.0 | 1.490 | 0.0000 | 0.6843 | 0.0000 |
| | 0.1 | 1.341 | -0.3620 | 0.6551 | -0.2070 |
| | 0.2 | 0.921 | -0.5621 | 0.4793 | -0.3559 |
| | 0.3 | 0.498 | -0.5573 | 0.2410 | -0.3711 |
| | 0.4 | 0.159 | -0.3110 | 0.0870 | -0.2705 |
| | 0.5 | 0.000 | 0.0000 | 0.0000 | 0.0000 |
| Konda and ardogan | 0.0 | 1.446 | 0.0000 | 0.6789 | 0.0000 |
| | 0.1 | 1.306 | -0.3411 | 0.6281 | -0.1950 |
| | 0.2 | 0.944 | -0.5339 | 0.4882 | -0.3288 |
| | 0.3 | 0.461 | -0.5628 | 0.4880 | -0.3921 |
| | 0.4 | 0.156 | -0.3137 | 0.0856 | -0.2637 |
| | 0.5 | 0.000 | 0.0000 | 0.0000 | 0.0000 |

*3.3 Edge crack in a functionally graded plate under shear traction loads*

In this section, an edge crack in a functionally graded plate under shear traction loads is considered (Fig. 7(a)). This problem has been studied by Dolbow and Gosz, with the following data: *H*/*W* = 16/7 and *a*/*W* = 0.5. As can be seen from the figure, the top edge is exposed to positive shear traction load, while the bottom horizontal edge is clamped [10]. Again, in an effort to simulate plane strain conditions, a one-layer finite element is generated containing 2346 20-noded hexahedral elements(Fig. 7(b))., and the nodes on the back and front faces of the model are restrained in "*z*" direction.

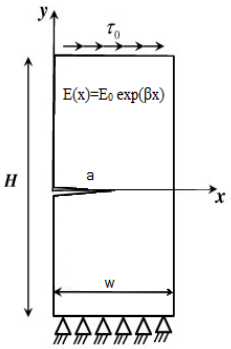


(a)

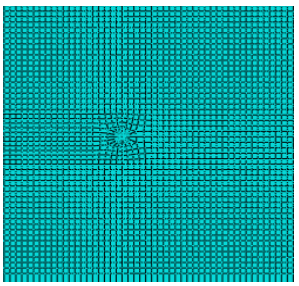

(b)

**Fig. 7**
(a) Edge crack in an FGM plate under remote shear traction load, (b) Finite element model.

The normalized mixed-mode stress intensity factors for different values of $E_2/E_1$ are shown in Fig. 8. $E_1$ and $E_2$ are the values of the elastic modulus at $x = 0$ and $x = W$, respectively. The elastic modulus varies according to $E(x) = E_0\, e^{\beta x}$. As can be seen from the figure, both mode-I and mode-II stress intensity factors decrease for increasing $E_2/E_1$ and that, mode-II component having slightly higher values, both modes of the stress intensity factor are close to each other. The normalizing stress intensity factors for each mode are the corresponding values for the case where $E_2/E_1 = 1$. Comparison of these results with those from Dolbow and Gosz (2002) shows excellent agreement between the two sets of solutions.

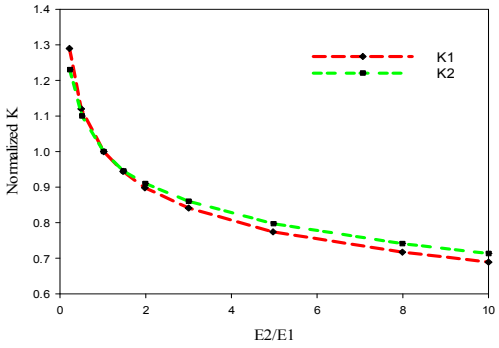


**Fig. 8**
Normalized mode-I and mode-II stress intensity factors for an edge crack contained in an FGM plate under remote shear traction load.

### *3.4 Deflected surface crack in a functionally graded plate under uniform tension*

Next, a deflected semi-elliptical surface crack in a finite-thickness FGM plate under uniform tensile loading is considered (Fig. 9). The elastic modulus varies according to $E(x) = E_0\, e^{\beta x}$ and poisson's ratio is constant (ϑ=0.25). As observed from the geometry and loading conditions of the problem, all three modes of fracture exist, and therefore it is a good example to test and demonstrate the accuracy of the method employed. The geometry details are; *a/c = 2, a/t = 0.8,* and total width and height of the plate are *4*t *(*Fig. 9).

The deflection angle of the crack from the "*x*-*z*" plane is 45°. Due to symmetry in "*z*" direction, only half of the geometry is modeled and therefore, all nodes on the symmetry plane are restrained in this direction. Fig. 10 shows the finite element model, which had a total of 125,176 quadratic 20-node hexahedral and 10-node tetrahedral elements. Along the crack front, 140 20-node hexahedral elements, or equivalently 281 nodes, are modeled. Fig. 11 shows the normalized mode-I stress intensity factor distribution along the crack front for two different material gradations, $E_2/E_1 = 20$ and $E_2/E_1 = 0.05$, and homogeneous material case. $E_1$ and $E_2$ are the values of the elastic modulus at $x = 0$ and $x = t$, respectively. Parametric angle definition is the same as those shown in Fig. 3. The stress intensity factors are normalized by Eqs. (15) and (16). A conclusion can not be drawn about the general behavior of

mode-I stress intensity factor along the whole crack front as the comparisons between different material cases change from one end of the crack front to the other. However, it can be said that the material property gradation has a big impact on the shape and magnitude of the mode-I stress intensity factor along the crack front. It should be noted that $\vartheta = 0^\circ$ corresponds to the free-surface, and no special attempt is made in the current analysis to capture the "correct" behavior of mixed-mode stress intensity factors at this location. However, the capabilities of studying the free-surface effects and prescribing constraints on the stress intensity factors to simulate correct behavior near the free-surface have been demonstrated. Similarly, Fig. 12 and Fig. 13 show the normalized mode-II and mode-III stress intensity factor distributions for different gradation and homogeneous material cases. It is seen that material gradation has considerable effect on mode-II and mode-III stress intensity factors also.

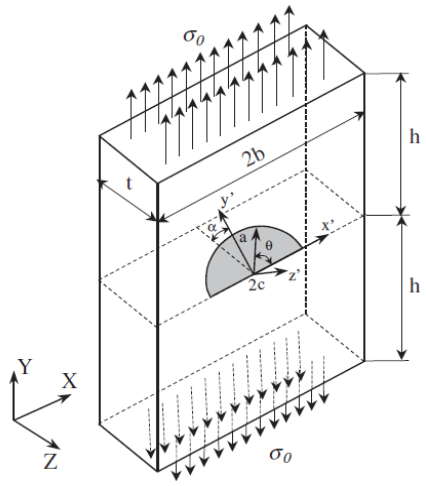


**Fig. 9**
Deflected surface crack in a functionally graded plate under uniform tension loading.

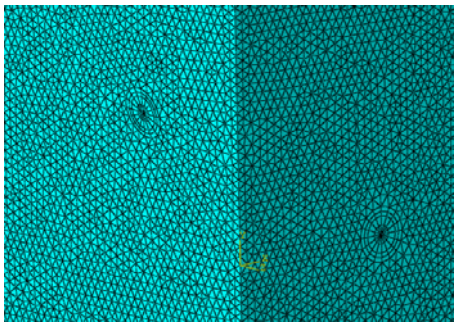

**Fig. 10**
Finite element model of a semi-elliptical deflected surface crack (a/c = 2) in a finite-thickness FGM plate, (Close-up view of crack region).

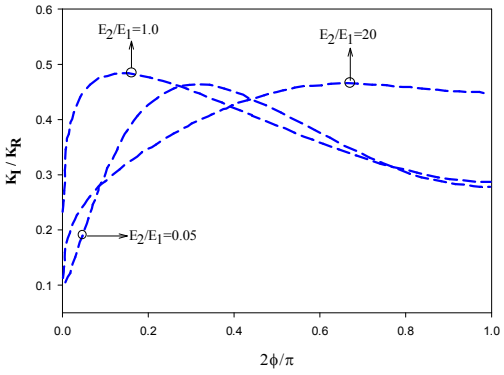


**Fig. 11**
Normalized mode-I stress intensity factors for a deflected semi-elliptical surface crack (a/c = 2) in a finite-thickness FGM plate.

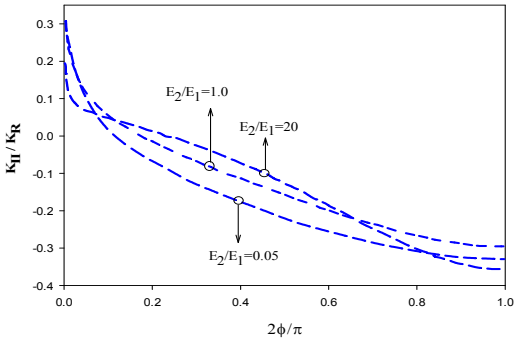


**Fig. 12**
Normalized mode-II stress intensity factors for a deflected semi-elliptical surface crack (a/c = 2) in a finite-thickness FGM plate.

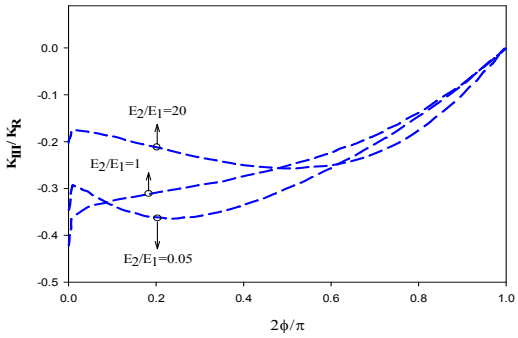


**Fig. 13**
Normalized mode-III stress intensity factors for a deflected semi-elliptical surface crack (a/c = 2) in a finite-thickness FGM plate.

## 4 CONCLUSIONS

The trend in simulation and analysis of mechanical behavior and fracture of functionally graded materials is going towards modeling the three-dimensional nature of geometry and loading. Thus, it is critical to have methods and tools, which are accurate and easy to use, to analyze the real three-dimensional fracture conditions in FGMs. The early analytical studies of two-dimensional cracks in FGMs, starting from 1983, helped develop finite element-based numerical methods to initially analyze two-dimensional mode-I and mixed-mode fracture problems in FGMs. More recently, three-dimensional finite element solutions for cracks in FGM structures, including the mixed-mode behavior, have also been reported in the literature. In this study, functionally graded enriched finite elements are developed and used to solve three-dimensional mixed-mode fracture problems in different FGM structures. A general-purpose finite element program, ABAQUS, is enhanced for this capability. It is shown that enriched finite elements allow accurate and efficient computation of fracture parameters, i.e., mixed-mode stress intensity factors, for elastic three-dimensional cracks in FGMs. Examples included various two and three-dimensional mixed-mode cracks, for which solutions from analytical and/or other numerical methods exist. Comparisons of current results with other methods show good agreement. Thus, it is concluded that the enriched elements can be applied to three-dimensional mixed-mode cracks in FGMs accurately and efficiently without needing special meshes near the crack front and detailed post-processing of the finite element solution.

## REFERENCES

[1] Ozturk M., Erdogan F., 1996, Axisymmetric crack problem in bonded materials with a graded interfacial region, *International Journal of Solids and Structures* **33**(2):193-219.

[2] Delale F., Erdogan F., 1983, The crack problem for a nonhomogeneous plane, *Journal of Applied Mechanics* **50**(3): 609-614.

[3] Eischen j.w., 1987, Fracture of nonhomogeneous materials, *International Journal of Fracture* **34**: 3-22.

[4] Konda N., Erdogan F., 1994, The mixed-mode crack problem in a nonhomogeneous elastic medium, *Engineering Fracture Mechanics* **47**(3): 533-545.

[5] Erdogan F., Wu B.H., 1997, The surface crack problem for a plate with functionally graded properties, *Journal of Applied Mechanics* **64**(1): 449-456.
[6] Honein T., Herrmann G., 1997, Conservation laws in nonhomogeneous plane elastostatics, *Journal of Mechanics and Physics of Solids* **45**(5): 789-805.
[7] Gu P., Dao M., Asaro R.J., 1999, A simplified method for calculating the crack-tip field of functionally graded materials using the domain integral, *Journal of Applied Mechanics* **66**(1): 101-108.
[8] Santare M.H., Lambros J., 2000, Use of graded finite elements to model the behavior of nonhomogeneous materials, *Journal of Applied Mechanics* **67**(4): 819-822.
[9] Kim J.H., Paulino G.H., 2002, Finite element evaluation of mixed mode stress intensity factors in functionally graded materials, *International Journal for Numerical Methods in Engineering* **53**(6): 1903-1935.
[10] Dolbow J.E., Gosz M., 2002, On the computation of mixed-mode stress intensity factors in functionally graded materials, *International Journal of Solids and Structures* **39**(2): 2557-2574.
[11] Kim J.H., Paulino G.H., 2002, Isoparametric graded finite elements for nonhomogeneous isotropic and orthotropic materials, *Journal of Applied Mechanics* **69**(4): 502-514.
[12] Anlas G., Lambros J., Santare M.H., 2002, Dominance of asymptotic crack tip fields in elastic functionally graded materials, *International Journal of Fracture* **115**(4): 193-204.
[13] Shim D.J., Paulino G.H., Dodds R.H., 2006, Effect of material gradation on K-dominance of fracture specimens, *Engineering Fracture Mechanics* **73**(4): 643-648.
[14] Walters M.C., Paulino G.H., Dodds R.H., 2004, Stress-intensity factors for surface cracks in functionally graded materials under mode-I thermomechanical loading, *International Journal of Solids and Structures* **41**(5): 1081-1118.
[15] Yildirim B., Dag S., Erdogan F., 2005, Three-dimensional fracture analysis of FGM coatings under thermomechanical loading, *International Journal of Fracture* **132** (4): 369-395.
[16] Walters M.C., Paulino G.H., Dodds R.H., 2004, Computation of mixed-mode stress intensity factors for cracks in three-dimensional functionally graded solids, *Journal of Engineering Mechanics* **132** (1): 1-15.
[17] Ayhan A.O., 2007, Mixed-mode stress intensity factors for deflected and inclined surface cracks in finite-thickness plates, *Engineering Fracture Mechanics* **71** (7):1059-1079.
[18] Ayhan A.O., Nied H.F., 2002, Stress intensity factors for three-dimensional surface cracks using enriched finite elements, *International Journal for Numerical Methods in Engineering* **54** (6): 899-921.
[19] Hartranft R.J., Sih G.C., 1969, The use of eigenfunction expansions in the general solution of three-dimensional crack problems, *Journal of Mathematics and Mechanics* **19**:123-138.